Cancer Cell
Article

Concomitant Pancreatic Activation of *Kras*^{G12D} and *Tgfa* Results in Cystic Papillary Neoplasms Reminiscent of Human IPMN

Jens T. Siveke,[1] Henrik Einwächter,[1] Bence Sipos,[2] Clara Lubeseder-Martellato,[1] Günter Klöppel,[2] and Roland M. Schmid[1,*]
[1]Department of Internal Medicine, Technical University of Munich, D-81675 Munich, Germany
[2]Department of Pathology, University Hospital Schleswig-Holstein, Campus Kiel, D-24105 Kiel, Germany
*Correspondence: roland.schmid@lrz.tum.de
DOI 10.1016/j.ccr.2007.08.002

SUMMARY

Growth factors have been implicated in pancreatic carcinogenesis. In this study we analyzed the effect of Tgfa overexpression in addition to mutant Kras^{G12D} by crossing Elastase-Tgfa mice with *p48*$^{+/Cre}$;*Kras*$^{+/LSL-G12D}$ mice. We show that concomitant expression of TGFα and *Kras*^{G12D} accelerates the progression of mPanIN lesions to metastatic pancreatic cancer and leads to the development of cystic papillary lesions resembling human intraductal papillary mucinous neoplasms (IPMN). Microarray data in mice revealed an IPMN signature and IPMNs expressed MUC1 and MUC5AC but not MUC2, similar to human pancreatobiliary IPMNs. Invasive ductal adenocarcinoma developed from PanINs and IPMNs, suggesting precursor lines for both lesion types in this model. In conclusion, Egfr signaling in synergy with oncogenic Kras may be a prerequisite for IPMN development and progression to pancreatic cancer.

INTRODUCTION

Pancreatic ductal adenocarcinoma (PDAC) has an overall 5-year-survival rate below 5% without substantial improvements within the last 20 years despite improving surgical and medical treatment modalities (Allison et al., 1998; Schneider et al., 2005; Warshaw and Fernandez-del Castillo, 1992). To date, three different precursor lesions for invasive pancreatic ductal adenocarcinoma (PDAC) have been described: pancreatic intraepithelial neoplasia (PanIN), intraductal papillary mucinous neoplasm (IPMN), and mucinous cystic neoplasm (MCN), with PanINs being the best characterized of these lesions (Brugge et al., 2004; Maitra et al., 2005). The identification and classification of PanINs as precursors of PDAC (Hruban et al., 2004) have led to the development of a morphological and genetic progression model of pancreatic cancer (overview in Hezel et al., 2006) and have facilitated the development of sophisticated genetically engineered mouse models for pancreatic cancer (Hruban et al., 2006). However, of multiple approaches, only mouse models with an endogenous *Kras*^{G12D} mutation recapitulated the full spectrum of human pancreatic carcinogenesis with murine PanIN (mPanIN) lesions progressing to PDAC (Guerra et al., 2003; Hingorani et al., 2003). While these mice develop metastasizing PDAC only at an advanced age, subsequent studies using mice with combinatorial conditional induction of *Kras*^{G12D} with either mutated *Tp53*^{R172H} or with loss of *p16/Ink4a*, *p19/Arf*, or *Tp53* have demonstrated that additional genetic alterations typically found in the human disease accelerate the carcinogenic process (Aguirre et al., 2003; Bardeesy

SIGNIFICANCE

Pancreatic ductal adenocarcinoma (PDAC) is thought to develop from PanIN, IPMN, and MCN preneoplastic lesions with PanIN lesions being the most prevalent and best-characterized precursors to pancreatic cancer. Cystic neoplasms are increasingly diagnosed, yet their management is challenged by their heterogeneity. IPMNs are among the most common cystic lesions; however, their molecular alterations and malignant potential are still largely unknown. We present here an endogenous model of PDAC in which cystic papillary tumors with strong resemblance to human IPMNs of the pancreatobiliary type develop. Moreover, these lesions progress to invasive cancer. In this model we provide evidence for different types of pancreatic precursor lesions developing in the same genetic background, thus enabling identification of common and alternating genetic alterations.

et al., 2006a; Hingorani et al., 2005). Interestingly, each additional genetic alteration led to different biological tumor features demonstrating the dependence of the phenotype and biological course of the resulting malignant tumors from the respective genotype (Siveke and Schmid, 2005). Of note, PDAC developed through PanIN lesions and not through IPMNs or MCNs suggesting that other factors or pathways may be important for the induction, progression, and malignant transformation of these particular precursor lesions. IPMN and MCN belong to a group of pancreatic cystic neoplasms that are increasingly recognized as relevant clinical entities (Furukawa et al., 2005; Kosmahl et al., 2004). While PanINs can now be excellently studied in mouse models, IPMN and MCN precursor lesions have been difficult to analyze with regard to their molecular properties and malignant potential partially due to the lack of suitable mouse models. In a recent study in which patients with an increased familial risk of developing PDAC were under intense medical observation, IPMNs were more often seen than advanced PanINs, suggesting that IPMN precursor lesions are a much more common part of the premalignant phenotypic spectrum (Canto et al., 2006). Recently, mouse models with concomitant conditional activation of Kras^{G12D} and heterozygosity or loss of Smad4 have been described in which MCN and IPMN lesions developed, suggesting that Smad4 plays an important and context-dependent role in cell fate, differentiation, and precursor lesion decisions (Bardeesy et al., 2006b; Izeradjene et al., 2007).

In addition to genetic alterations in *CDKN2/INK4A*, *TP53*, or *DPC4/SMAD4*, substantial evidence from human and murine PDAC studies implies an important role of growth factor signaling in the carcinogenic process (Barton et al., 1991; Friess et al., 1999). In an early mouse model studying the role of *Tgfa* in the pancreas, mice with transgenic overexpression of TGFα under control of the pancreatic Elastase promoter (*Ela-Tgfa*), acino-ductal transdifferentiation, and at advanced age, development of PDAC with similar genetic alterations as those found in humans was demonstrated (Sandgren et al., 1990; Wagner et al., 1998, 2001). However, these mice did not develop PDAC through well-defined premalignant mPanIN lesions. In an effort to study the role of Egfr signaling in pancreatic carcinogenesis, we have combined two mouse models for PDAC, *Ela-Tgfa* transgenic mice and conditional *p48*$^{+/Cre}$;*Kras*$^{+/LSL\text{-}G12D}$ mice for generating *p48*$^{+/Cre}$;*Kras*$^{+/G12D}$;*Ela-Tgfa* mice.

RESULTS

Kras^{G12D};*Ela-Tgfa* Mice Develop Cystic Papillary Neoplasms

To develop a model of PDAC minimizing the risk of acquiring extrapancreatic oncogenic pathologies, *Kras*$^{+/LSL\text{-}G12D}$ mice were crossed to pancreas-specific *p48*$^{+/Cre}$ mice, which have been generated in our lab (Nakhai et al., 2007; *p48*$^{+/Cre}$; *Kras*$^{+/LSL\text{-}G12D}$ will be termed *Kras*^{G12D} hereafter). *Ptf1a*, also known as *p48*, is required for commitment of all pancreatic lineages and specifying an exocrine cell fate. These mice, as expected, revealed essentially the same preneoplastic and malignant features as mice described by Hingorani et al. (Hingorani et al., 2003). Induction and progression of CK19$^+$ and MUC5AC$^+$ mPanIN lesions to metastatic PDAC occurred as reported, and pancreas-specific recombination was confirmed using a Rosa26r^{lacZ} reporter mouse (see Figure S1 in the Supplemental Data available with this article online), demonstrating that our *p48*$^{+/Cre}$ mice function in a manner similar to previously reported *p48/Ptf1a-Cre* mice (Kawaguchi et al., 2002). To analyze the effect of concomitant expression of mutated *Kras*^{G12D} and TGFα, we crossed *Kras*^{G12D} mice with *Ela-Tgfa* mice. *Kras*^{G12D};*Ela-Tgfa* mice were born at expected Mendelian ratios and grew to adulthood without visible phenotypic abnormalities making them indistuingishable from wild-type (WT), *Kras*^{G12D}, and *Ela-Tgfa* littermates.

When *Kras*^{G12D};*Ela-Tgfa* mice were analyzed at 2 to 3 months of age, we observed a severely altered pancreas compared to littermate genotypes with small and large cysts and various types of ductal lesions. Acino-ductal metaplasia, mPanIN, and cystic papillary lesions had almost completely replaced the acinar tissue (Figures 1A and 1B). mPanIN lesions ranged from mPanIN-1A to −2 lesions. We also noted some mPanIN-3 lesions, which sometimes had a cystic appearance (Figures 1C–1F). These high-grade lesions are almost never seen in *Kras*^{G12D} pancreata at this age, suggesting an accelerated mPanIN progression. Interestingly, in addition to acino-ductal and mPanIN lesions, we noticed a third type of lesion characterized by papillary cell proliferations which had formed in branches of the main pancreatic duct (Figures 1G–1I). Mucin production by these cystic papillary lesions was demonstrated by PAS staining (Figure 1J). When compared with two mucin-producing cystic neoplasms of the human pancreas, MCN and IPMN, the mouse cystic papillary neoplasms resembled more closely human IPMNs than MCNs because of the lack of ovarian-like stroma (Hruban et al., 2006).

Cystic Papillary Lesions of *Kras*^{G12D};*Ela-Tgfa* Mice Do Not Originate from Differentiated Acinar Cells

To prove that the cystic papillary lesions derive from p48$^+$ cells, we crossed *Rosa26r*^{lacZ} reporter mice with *Kras*$^{+/G12D}$;*Ela-Tgfa* mice. As expected, we found these papillary lesions to originate from p48$^+$ cells (Figure 2A), suggesting that they derive from either pancreatic stem, acinar, or duct-like cells. To test whether these cystic papillary lesions were also inducible in PDX1$^+$ cells, *Pdx1-Cre*; *Kras*$^{+/G12D}$;*Ela-Tgfa* mice were analyzed at 3 months of age, at which both mPanIN and cystic papillary lesions were detected (data not shown) supporting the hypothesis that both preneoplastic lesions may originate from a common precursor cell and not from a terminally differentiated acinar cell.

We next addressed the hypothesis whether acinar cells are potential precursors of IPMN-like lesions. Therefore, we replaced *p48*$^{+/Cre}$ mice by *Elastase-Cre-ER* mice for

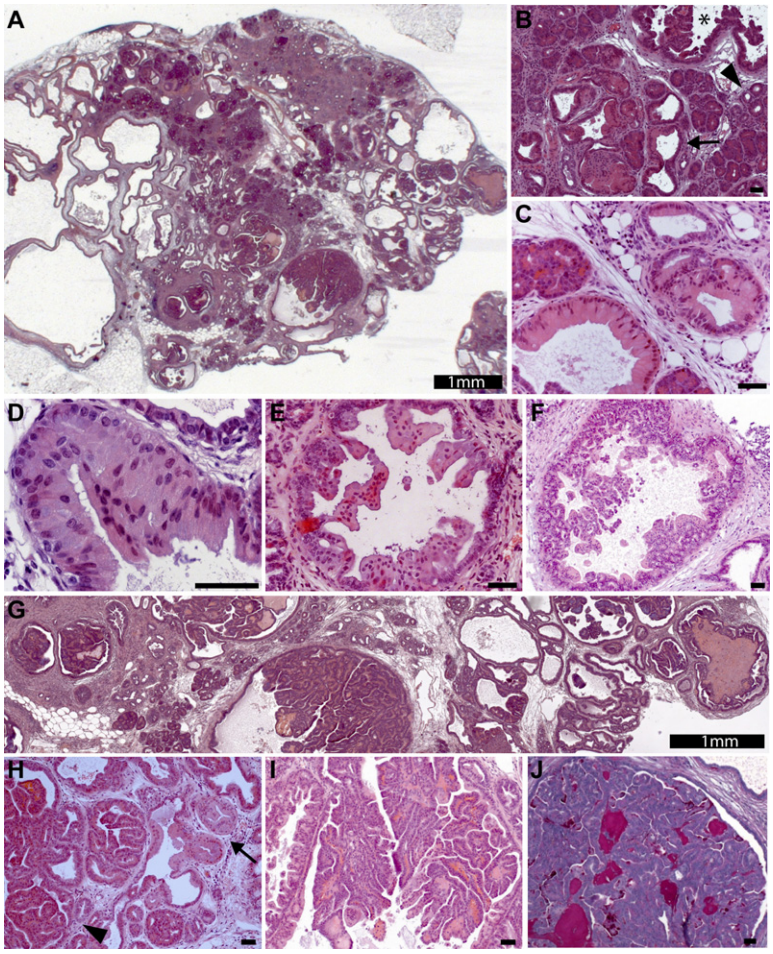

Figure 1. Histology of Different Ductal Lesions in *Kras*^{G12D};*Ela-Tgfa* Mice

(A) Gross morphology reveals replacement of acinar tissue by cysts and various small and large ductal structures.

(B) Acinoductal metaplasia (arrowhead), mPanIN (arrow), and cystic papillary lesions (*) are present.

(C–F) mPanIN1A+B (C), 2 (D), −3 (E) and cystic mPanIN3 (F) lesions.

(G–I) *Kras*^{G12D};*Ela-Tgfa* pancreata (G) contain small (H, arrowhead) and large (I) cystic papillary lesions with adjacent mPanINs (H, arrow).

(J) PAS stain reveals high mucin content in cells of papillary lesions.

Mice are 9–13 weeks of age; scale bar is 50 μm or as shown.

induction of *Kras*^{G12D} expression. By an additional crossing, we generated *Ela-Cre-ER;Kras*^{G12D}*;Ela-Tgfa* mice with the *Rosa26r*^{lacZ} allele for monitoring of Tamoxifen (TM)-induced Cre recombination and cell lineage tracing. Application of multiple TM injections 4 weeks after birth induced widespread Cre-dependent recombination in *Ela-Cre-ER;Kras*^{G12D}*;Ela-Tgfa*;*Rosa26r*^{lacZ} mice 4 and 15 weeks after injections as examined by positive X-gal staining of acinar but not ductal or islet cells, whereas only very few if any acinar cells were X-gal positive in vehicle-treated animals (Figure 2B and data not shown). To analyze the induction of mPanIN and/or IPMN-like lesions, four *Ela-Cre-ER;Kras*^{G12D}*;Ela-Tgfa*;*Rosa26r*^{lacZ} mice were followed for 15 weeks. In three of these animals, we found acino-ductal metaplasia and only rarely mPanIN1 lesions, although mPanIN1 lesions were sometimes difficult to distinguish from acino-ductal metaplasia (Hruban et al., 2006). Interestingly, one mouse showed formation of very few small-sized IPMN-like lesions (Figure 2C). To further validate the hypothesis whether cystic papillary lesions from *Kras*^{G12D};*Ela-Tgfa* mice may originate from acinar cells or acino-ductal metaplasia, we used double-immunofluorescence for amylase and CK19 to identify potential double-positive cystic papillary lesions. When double-immunofluorescence for amylase and CK19 was applied to *Kras*^{G12D};*Ela-Tgfa* pancreata at different stages of carcinogenesis, we found tubular complexes with acino-ductal metaplasia staining positive for acinar and ductal marker as expected (Figures 2D and 2E). However, we failed to observe clear double-positive cells within IPMN-like lesions. In fact, most IPMNs like mPanINs were CK19 single-positive, although amylase single-positive cells were infrequently found in IPMN-like lesions (Figure 2E and 2F). Thus, while these data do not prove a ductal or progenitor cell as precursor of IPMN-like lesions, we found this lesion type to be clearly distinguishable from acino-ductal metaplastic lesions. We next sought to examine IPMN-like lesions with regard to pathways involved in specification of embryonic and adult pancreatic cell fate. As activation of hedgehog signaling was recently reported in human IPMNs and mPanIN lesions (Ohuchida et al., 2006; Hingorani et al., 2003), we investigated the expression of SHH. While we observed SHH-positive mPanIN lesions in *Kras*$^{+/G12D}$;*Ela-Tgfa* mice, we found no definite expression in IPMN-like lesions at 9–13 weeks of age (Figure 2G). Moreover, we found no increased expression of the Hedgehog target genes Gli1 and Gli2 in *Kras*$^{+/G12D}$;*Ela-Tgfa* pancreata compared to littermate controls as determined by qRT-PCR in pancreatic mRNA of young animals 7 days of age (data not shown),

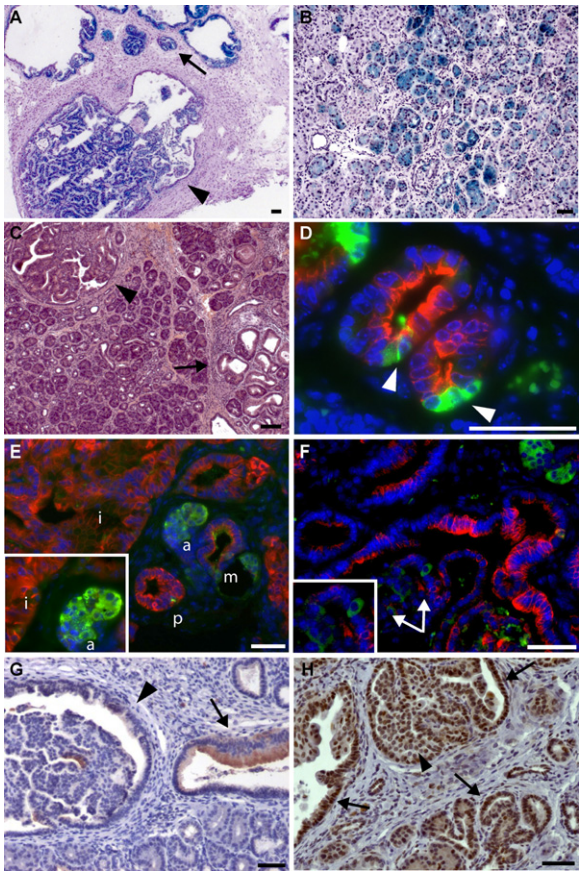

Figure 2. Immunohistochemical Analysis of Cystic Papillary Lesions in *Kras*^{G12D};*Ela-Tgfa* Mice

(A) mPanIN (arrow) and cystic papillary lesions (arrowhead) are X-gal positive in *Kras*^{G12D};*Ela-Tgfa*;*Rosa26r*^{lacZ} reporter mice demonstrating Cre-induced recombination in both lesion types.

(B) Acinar, but not islet and ductal cells, are X-gal positive 15 weeks after Tamoxifen-induced Cre recombination in *Ela-Cre-ER*;*Kras*^{G12D};*Ela-Tgfa*;*Rosa26r*^{lacZ} mice.

(C) Formation of mPanIN (arrow) and cystic papillary lesions (arrowhead) in *Ela-Cre-ER*;*Kras*^{G12D};*Ela-Tgfa* mice 15 weeks after induction.

(D) Double-immunofluorescence for amylase (green) and CK19 (red) reveals double-positive cells within tubular complexes with acinoductal metaplasia (arrowhead).

(E) While many IPMNs (i) and PanINs (p) are CK19 single-positive, acino-ductal metaplastic lesions (m) next to acini (a) express amylase.

(F) Amylase-positive cells can be found in IPMN-like lesions. Nuclei were counterstained with DAPI. Mice are 18 weeks of age.

(G) Shh staining reveals expression in mPanIN (arrow), but not cystic papillary lesions (arrowhead), of *Kras*^{G12D};*Ela-Tgfa* mice.

(H) HES1 expression is high in mPanIN and cyst-lining cells (arrows) with lower expression in papillary cells of cysts (arrowhead).

Analysis of *Kras*^{G12D};*Ela-Tgfa* mice at 9 weeks of age or as noted. Scale bar, 50μm.

a time at which many genes implicated in IPMN carcinogenesis are already detectable (see below). Thus, these data suggest that Hedgehog signaling has no prominent role in IPMN lesion formation in this model. Finally, we investigated the involvement of Notch signaling in IPMN-like lesions. Activation of this pathway can be assessed by nuclear expression of the Notch signaling target gene HES1. Importantly, centroacinar cells, which are thought to represent pancreatic progenitor cells, are characterized by nuclear expression of HES1 and have been implicated as cells of origin of ductal tumors (Stanger et al., 2005). To define the role of Notch activation and centroacinar cells as potential source of preneoplastic lesions in *Kras*^{G12D};*Ela-Tgfa* mice, we analyzed the amount and localization of HES1 positive cells at different time points. As described previously, we found HES1 expression to be restricted to centroacinar cells in normal pancreata and in mPanIN lesions of *Kras*^{G12D} mice at 7 days and 3 months of age (Figures S2A and S2B). While we did not observe HES1 expression in *Ela-Tgfa* pancreata, *Kras*^{G12D};*Ela-Tgfa* mice showed strong and early expression of HES1 in exocrine cells at 7 days (Figure S2C). In older mice with distinct preneoplastic lesions, HES1 expression was found in cells of acino-ductal metaplastic structures, mPanIN and cystic papillary lesions (Figure S2D). Regarding expression in cystic papillary lesions, HES1 expression was observed in the flat cystic epithelium surrounding the papillary proliferations as well as in the papillary lesions themselves, suggesting a role for Notch signaling activation during IPMN lesion development (Figure 2H).

Immunohistochemical Analysis of the Cystic Papillary Lesions Reveals Key Characteristics of Human IPMNs of the Pancreatobiliary Type

Human IPMNs can be divided into four main types based on morphological features and the expression of MUC1, MUC2, MUC5AC, and CDX2 as recently described (Furukawa et al., 2005). Thus, we performed immunohistochemical staining for MUC1, 2, and 5AC in sections of *Kras*$^{+/G12D}$;*Ela-Tgfa* mice 3 months of age and in sections from human patients presenting with IPMNs (Figure 3). While IPMN-like lesions from *Kras*$^{+/G12D}$;*Ela-Tgfa* mice were MUC1- and MUC5AC-positive, there was no immunohistochemical reactivity for MUC2 and CDX2 (Figure 3 and Figure S3A). This pattern corresponds to the pancreatobiliary type of human IPMNs. A ductal phenotype was demonstrated by CK19 expression (Figures 2E and 2F) since amylase and insulin staining was negative apart from islets trapped within the cystic lesions (Figures 2E and 2F and Figure S3B). We next analyzed the expression of PDX1, which revealed nuclear expression in mPanIN lesions in cells lining the cysts and in cells of the cystic papillary lesions demonstrating the pancreatic origin of these cells (Figure S3C).

Cystic papillary lesions have also been observed in other mouse models of PDAC including *Ela-Kras*^{G12D}, *Mist1-Kras*^{G12D}, and *Ptf1a-Cre LSL-Kras*^{G12D} *Smad4*$^{lox/lox}$ mice (Bardeesy et al., 2006b; Grippo et al., 2003; Tuveson et al., 2006). Interestingly, cystic papillary lesions can also be found in *Ela-Tgfa* mice albeit at low frequency and at advanced age (less than 3% of *Ela-Tgfa* mice older than one year of age; J.T.S., unpublished data). To evaluate whether these cystic lesions show similarities to IPMN-like lesions from *Kras*$^{+/G12D}$;*Ela-Tgfa* mice, sections of cystic papillary lesions from *Ela-Tgfa* transgenic animals were analyzed by immunohistochemistry. While CK19,

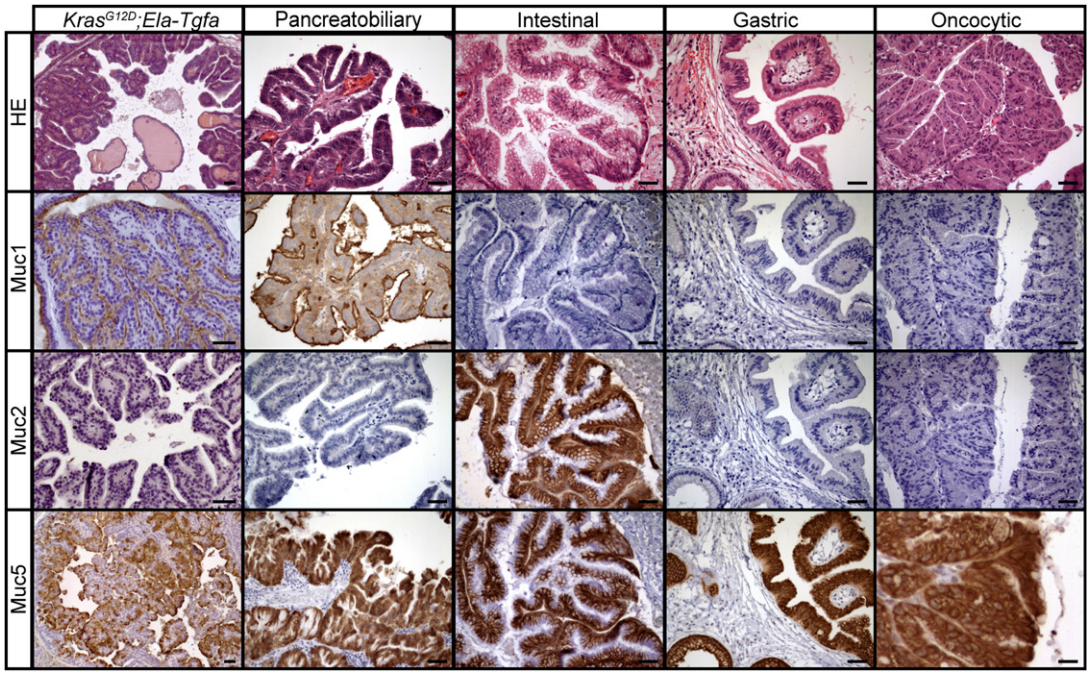

Figure 3. Cystic Papillary *Kras*^{G12D};*Ela-Tgfa* Lesions Show Characteristics of Human Pancreatobiliary IPMNs
Kras^{G12D};*Ela-Tgfa* pancreata and different human IPMNs were stained with H&E or for MUC1, MUC2, and MUC5AC. *Kras*^{G12D};*Ela-Tgfa* pancreata 9–12 weeks of age show similar MUC expression patterns as human pancreatobiliary IPMNs compared to gastric, intestinal, and oncocytic IPMNs. Scale bar, 50μm.

MUC1, and MUC5AC were expressed, albeit at lower levels than in *Kras*$^{+/G12D}$;*Ela-Tgfa* lesions, no expression of MUC2 and CDX2 was notable (Figures S3D–S3F and data not shown).

Development of Preneoplastic Lesions in *Kras*^{G12D};*Ela-Tgfa* Pancreata

To evaluate the role of *Kras*^{G12D} and *Tgfa* for early preneoplastic alterations, we chose 7 days and 35 days for analysis of the carcinogenic process (7 days and 35 days). At 7 days, WT and *Kras*^{G12D} pancreata were macroscopically of similar size and appearance, while pancreata of *Ela-Tgfa* and *Kras*^{G12D};*Ela-Tgfa* mice were significantly enlarged (data not shown). Histologically, WT and *Kras*^{G12D} pancreata were indistinguishable revealing no preneoplastic lesions, while *Ela-Tgfa* and at higher extent *Kras*^{G12D};*Ela-Tgfa* pancreata revealed duct-like structures and acino-ductal metaplasia (Figures 4A–4C). However, no mPanIN or cystic papillary lesions were detected in *Kras*^{G12D};*Ela-Tgfa* mice at this age. As *Ela-Tgfa* mice develop acino-ductal metaplasia, expression of acinar cell-defining genes was analyzed by qRT-PCR, which revealed a strong and synergistic reduction of acinar cell defining genes such as *p48* and *Elastase* (Figure S4A).

We next analyzed littermate mice at 35 days after birth at which in accordance with previous data few mPanIN-1 lesions and duct-like structures had formed in *Kras*^{G12D} and *Ela-Tgfa* mice, respectively. In contrast to this, *Kras*^{G12D};*Ela-Tgfa* mice showed a severe loss of acinar cells along with formation of mPanIN-1 and -2 as well as cystic papillary lesions, suggesting that development of preneoplastic lesions starts between 7 and 35 days after birth (Figures S4B–S4E).

Molecular Characterization of Precursor Lesions of *Kras*^{G12D};*Ela-Tgfa* Mice

To further characterize the evolving lesions of *Kras*^{G12D};*Ela-Tgfa* pancreata on a molecular level, whole pancreatic cell mRNA was prepared for genomic profiling at 7 days when precursor lesions had not yet developed. As pancreata of *Ela-Tgfa* and *Kras*^{G12D};*Ela-Tgfa* mice were significantly larger than wild-type and *Kras*^{G12D} pancreata showing increased proliferation as determined by Cyclin D1 staining (Figure 4D), we expected to identify a proliferation signature in these genotypes. Indeed, when we compared expression values of genes of a common proliferation signature (Perou et al., 1999), we clearly observed higher expression of most genes in *Ela-Tgfa* and *Kras*^{G12D};*Ela-Tgfa* pancreata (Figure 4E). We next tested the presence of a proliferation signature by gene set enrichment analysis (GSEA). GSEA evaluates a query microarray data set by using a collection of gene sets (Subramanian et al., 2005). As expected, we found a significantly upregulated GSEA score for proliferation in *Ela-Tgfa* and *Kras*^{G12D};*Ela-Tgfa* pancreata demonstrating the feasibility of this analysis for detection of pathway signatures (Figure 4F).

To test if *Kras*^{G12D};*Ela-Tgfa* pancreata at this age reveal an IPMN signature, we used a set of genes that was identified in a recent study to be specifically overexpressed in human IPMNs compared to normal pancreatic ductal

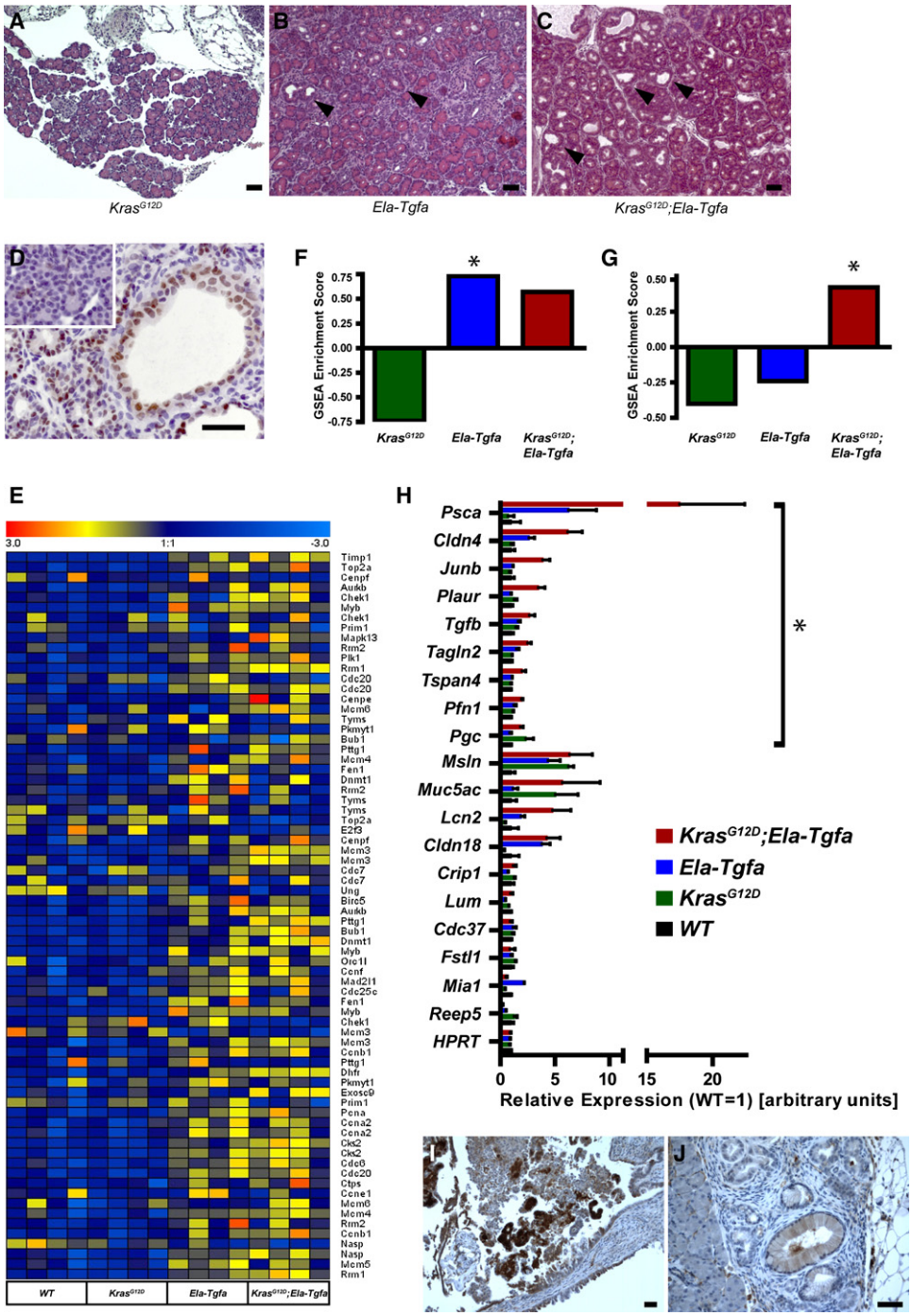

Figure 4. Proliferation and IPMN Signature in Early *Kras*^{G12D};*Ela-Tgfa* Pancreata

(A–C) Histology of *Kras*^{G12D} (A), *Ela-Tgfa* (B), and *Kras*^{G12D};*Ela-Tgfa* (C) pancreata demonstrates beginning acinoductal metaplasia but no precursor lesions in 7 day *Ela-Tgfa* and *Kras*^{G12D};*Ela-Tgfa* mice (arrowhead).

(D) Cyclin D1 is highly expressed in exocrine cells of 7 day *Kras*^{G12D};*Ela-Tgfa* mice. Insert shows lower expression in *Kras*^{G12D} mice.

(E) Image intensity display of expression levels of genes commonly activated during proliferation.

(F) GSEA analysis of *Kras*^{G12D}, *Ela-Tgfa*, and *Kras*^{G12D};*Ela-Tgfa* pancreata 7 days of age for the known set of genes upregulated during proliferation.

(G) GSEA analysis of *Kras*^{G12D}, *Ela-Tgfa*, and *Kras*^{G12D};*Ela-Tgfa* pancreata 7 days of age for the known set of genes upregulated in human IPMN tumors.

(H) Real-time quantitative RT-PCR of genes known to be upregulated in human IPMNs in 7 day pancreata of *Kras*^{G12D};*Ela-Tgfa* mice. Genes marked were significantly increased compared to wild-type controls (*$p < 0.05$; wild-type set to 1; results are expressed as mean; error bars indicate SEM, n = 3).

(I and J) Detection of PSCA expression in cystic papillary lesions (I) of *Kras*^{G12D};*Ela-Tgfa* mice but not in an early mPanIN lesion (J) of *Kras*^{G12D} mice (9 weeks of age). Scale bar, 50μm.

epithelial cells (Sato et al., 2004). Using this data set, a score defined from the IPMN defining genes was calculated for all four genotypes (WT, *Kras*^{G12D}, *Ela-Tgfa*, and *Kras*^{G12D}*;Ela-Tgfa*). While no significant differences were notable between WT, *Kras*^{G12D}, and *Ela-Tgfa* pancreata, there was a markedly higher score in *Kras*^{G12D}*;Ela-Tgfa* pancreata (Figure 4G and Figure S5), suggesting that, indeed, concomitant activation of *Kras*^{G12D} and Egfr signaling may be required for IPMN development.

To verify this signature we chose a random set of 21 genes upregulated in human IPMNs for analysis in real-time qRT-PCR. As shown in Figure 4H, 9 of 21 genes were significantly increased in *Kras*^{G12D};*Ela-Tgfa* mice compared to WT pancreata and 8 of these 9 genes were also significantly increased compared to *Kras*^{G12D} pancreata, suggesting a potential involvement in IPMN pathogenesis.

As *Psca* expression was highly increased we next determined its tissue expression by immunohistochemistry. Notably, expression of PSCA was seen predominantly in cystic papillary lesions of *Kras*^{G12D};*Ela-Tgfa* pancreata, but not in early mPanIN lesions of *Kras*^{G12D} mice (Figures 4I and 4J), correlating with the gene expression results.

Activation of Egfr and Stat3 in *Kras*^{G12D}*;Ela-Tgfa* Pancreata

We next analyzed Ras and Egfr-dependent effector signaling pathways in the early carcinogenic process. Analysis at 7 days revealed increased phosphorylation of EGFR and *HER2*/neu and increased *Egfr* and *Tgfa* mRNA expression in *Ela-Tgfa* and *Kras*^{G12D};*Ela-Tgfa* pancreata (Figures 5A and 5B). Immunohistochemical analysis revealed a variable expression of EGFR in some but not all IPMN-like lesions of *Kras*^{G12D};*Ela-Tgfa* mice (Figure 5C). Although we found RAS activation in *Kras*^{G12D} and at higher levels in *Kras*^{G12D};*Ela-Tgfa*, but not in WT and *Ela-Tgfa* pancreatic lysates by RAS activity assay (data not shown), we observed elevated levels of the phophorylated RAS effector ERK1/2 only in *Ela-Tgfa* and *Kras*^{G12D};*Ela-Tgfa*, but not in *Kras*^{G12D} pancreatic lysates, suggesting that TGFα-dependent EGFR signaling is involved in ERK1/2 activation at this early stage (Figure 5A). Correlating with the results from western blot analysis, we found increased ERK1/2 activation by immunohistochemical analysis (Figure 5D). Interestingly, no significant upregulation of phosphorylated p38 or AKT was noted in any littermates in western blot and immunohistochemical analysis, suggesting that not all Egfr or Ras-dependent signaling pathways are activated in *Kras*^{G12D};*Ela-Tgfa* mice (Figure 5A and data not shown). However, PTEN levels were slightly increased in *Kras*^{G12D};*Ela-Tgfa* pancreatic lysates, suggesting that the Akt-signaling pathway may nonetheless be involved in *Kras*^{G12D};*Ela-Tgfa* carcinogenesis (Figure 5A). We next analyzed phosphorylation of STAT3, a typical Egfr signaling target, which has been shown to play a role in pancreatic carcinogenesis (Greten et al., 2002; Miyatsuka et al., 2006). Here, we found upregulation of STAT3 phosphorylated at Tyr705 only in *Kras*^{G12D};*Ela-Tgfa* pancreatic lysates suggesting selective Stat3 pathway activation through concomitant Egfr and Kras^{G12D} signaling (Figure 5A). Moreover, we found upregulation of *Socs3*, a downstream mediator of Stat3, in *Kras*^{G12D};*Ela-Tgfa* pancreatic mRNA at 7 days supporting the hypothesis of functional Stat3 signaling (Figure 5B). Importantly, both phosphorylated STAT3 protein and *Stat3* and *Socs3* mRNA were highly increased in *Kras*^{G12D};*Ela-Tgfa*, but not *Ela-Tgfa* pancreata, suggesting a synergistic effect of Egfr and Kras signaling in Stat3 activation. Immunohistochemical analysis revealed a highly increased expression of phospho-STAT3 in *Kras*^{G12D};*Ela-Tgfa* pancreata at 7 days but not in control littermates (Figures S2E–S2H). At 9 weeks of age, phospho-STAT3 was found in nuclei of preneoplastic IPMN-like cells of *Kras*^{G12D};*Ela-Tgfa* (Figure 5F) as well as in some mPanIN lesions and surrounding acinar cells of *Kras*^{G12D} mice (Figure 5E). In older *Kras*^{G12D};*Ela-Tgfa* mice, expression was not confined to IPMN-like lesions but was also found in mPanIN and malignant ductal lesions (data not shown).

As Stat3 has been shown to prevent apoptosis, we next evaluated levels of the well-known Stat3 target gene *Bcl-xL*. We found Bcl-xL protein and mRNA expression to be selectively increased in *Kras*^{G12D};*Ela-Tgfa* pancreata, while the Bcl family member Bcl-2 was equally expressed in all littermates (Figures 5A and 5B), supporting a functional role for Stat3-induced inhibition of apoptosis in *Kras*^{G12D};*Ela-Tgfa* carcinogenesis. When 7 day microarray data sets were evaluated using a *Stat3* gene set from the Signal Transduction Knowledge Environment (STKE), we found a high GSEA score in the *Kras*^{G12D};*Ela-Tgfa* data set but not in any littermates (data not shown).

Survival Analysis and Histological Progression of *Kras*^{G12D}*;Ela-Tgfa* Precursor Lesions

As described above, *Kras*^{G12D};*Ela-Tgfa* pancreata revealed mPanIN precursor lesions and cystic papillary lesions similar to human IPMNs. Thus, we wondered whether both types of precursor lesions contribute to the development of invasive PDAC. Since we noted mPanIN-2 and occasionally mPanIN-3 lesions in animals 3 months of age, an age at which these lesions are only rarely found in *Kras*^{G12D} animals (Hingorani et al., 2005), we expected to observe an earlier development of PDAC. Indeed, *Kras*^{G12D};*Ela-Tgfa* mice had an increased incidence of invasive PDAC with a median survival of approximately 7 months, significantly shorter than that of *Kras*^{G12D} or *Ela-Tgfa* mice (Figure 6A; $p < 0{,}003$). Tumors seen were usually large and more often had a cystic appearance than PDAC from *Kras*^{G12D} mice. We observed a predominantly glandular tumor phenotype in most of the animals with mPanIN lesions surrounding invasive tumor cells, suggesting that these tumors originated from mPanIN lesions (Figure 6B). Disseminated metastases were found in about 50% of PDAC, predominantly in liver, lung, peritoneum, and lymph nodes (Figure 6C and 6D and data not shown).

Interestingly, we also observed progression of cystic papillary lesions in a substantial fraction of animals (20%–30%). In these mice, large intraductal cystic

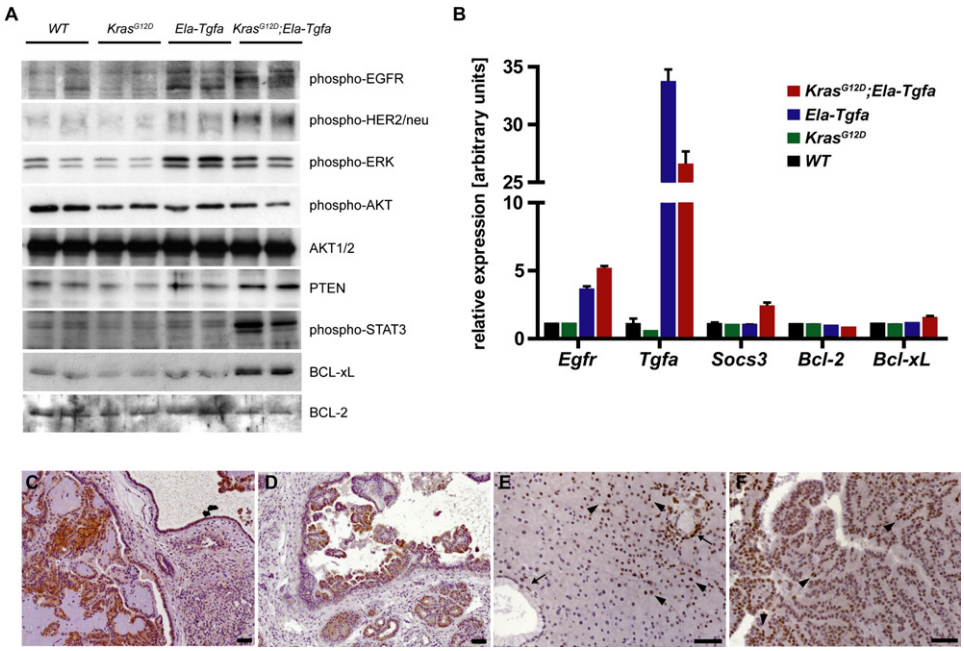

Figure 5. Egfr and Stat3 Signaling Pathways Are Activated in Early *Kras*^{G12D};*Ela-Tgfa* Carcinogenesis

(A) Protein expression of members of the Egfr, Ras, and Bcl-2 signaling pathways in representative 7 day pancreata of wild-type, *Kras*^{G12D}, *Ela-Tgfa*, and *Kras*^{G12D};*Ela-Tgfa* mice.

(B) Expression of Egfr, Stat3, and Bcl-2 signaling members by Affymetrix gene analysis shows increased expression in *Kras*^{G12D};*Ela-Tgfa* pancreata at 7 days (arbitrary units; wild-type set to 1; results are expressed as mean; error bars indicate SEM, n = 3).

(C and D) IPMN-like lesions from *Kras*^{G12D};*Ela-Tgfa* mice at 9 weeks of age show expression of EGFR (C) and phosphorylated ERK1/2 (D).

(E and F) Phosphorylated STAT3 is expressed in some nuclei of mPanIN lesions (arrows) and surrounding acinar cells (arrowheads) of *Kras*^{G12D} mice (E) as well as in many cells of IPMN-like lesions from *Kras*^{G12D};*Ela-Tgfa* mice at 6 months of age (F, arrowheads). Scale bar, 50 μm.

papillary neoplasms with almost complete absence of mPanIN lesions were present showing an IPMN-like phenotype. These large IPMN-like lesions exhibited nuclear atypia and a high proliferation rate as well as evidence for invasion (Figures 6E–6G). One animal with a tumor composed of IPMN-like lesions revealed invasion of the duodenum (Figures 6H and 6I). As we did not note any mPanINs or ductal complexes in this pancreas, invasive growth of cystic papillary cells into the duodenum seems very likely. In another mouse we noted large IPMN-like lesions invading the kidney and spleen (Figure 6J and data not shown). We also observed metastatic lesions with cystic appearance in the lung and liver suggesting that the metastases shared the cystic papillary features of the primaries. In conclusion, *Kras*^{G12D};*Ela-Tgfa* mice develop invasive and metastatic PDAC significantly earlier than *Kras*^{G12D} mice. These cancerous lesions are either accompanied by mPanIN lesions or by IPMN-like lesions suggesting that PDAC in *Kras*^{G12D};*Ela-Tgfa* mice originates from two types of PDAC precursor lesions.

Signaling Pathways in Different Subtypes of Human IPMNs

Given the activation of Egfr, Stat3, and Hes1 in *Kras*^{G12D};*Ela-Tgfa* preneoplastic and malignant IPMNs, we evaluated expression of EGFR, HER2/neu, phospho-STAT3, phospho-ERK, phospho-AKT, and HES1 in human IPMN subtypes. For this analysis, three IPMNs of either pancreatobiliary, intestinal, gastric, or oncocytic subtype were evaluated for expression by immunohistochemistry (Figure 7A). While we noted EGFR expression only in one pancreatobiliary and one oncocytic IPMN, HER2/neu and phospho-ERK were not detected. Phospho-AKT was expressed in only one pancreatobiliary but all intestinal and oncocytic IPMNs, suggesting a pathogenetic role in these subtypes. Phosphorylated STAT3 was found in all three pancreatobiliary IPMNs, albeit at varying levels and in one of three tumors in the other subtypes, respectively (Figure 7B). HES1 expression was found in one pancreatobiliary (Figure 7C) and one oncocytic IPMN but was not detected in intestinal and gastric IPMNs. Thus, while this analysis is preliminary, phospho-STAT3 and HES1 may be involved in the carcinogenesis of pancreatobiliary IPMNs.

DISCUSSION

To study the effect of increased Tgfa-induced Egfr signaling in an endogenous mouse model of PDAC, we have crossed TGFα-overexpressing mice with *Kras*$^{+/LSL-G12D}$ mice, two well-described murine models of human PDAC (Hingorani et al., 2003; Wagner et al., 2001; Wagner et al., 1998). The *Kras*$^{+/LSL-G12D}$ model was the first mouse model showing induction and progression of mPanIN

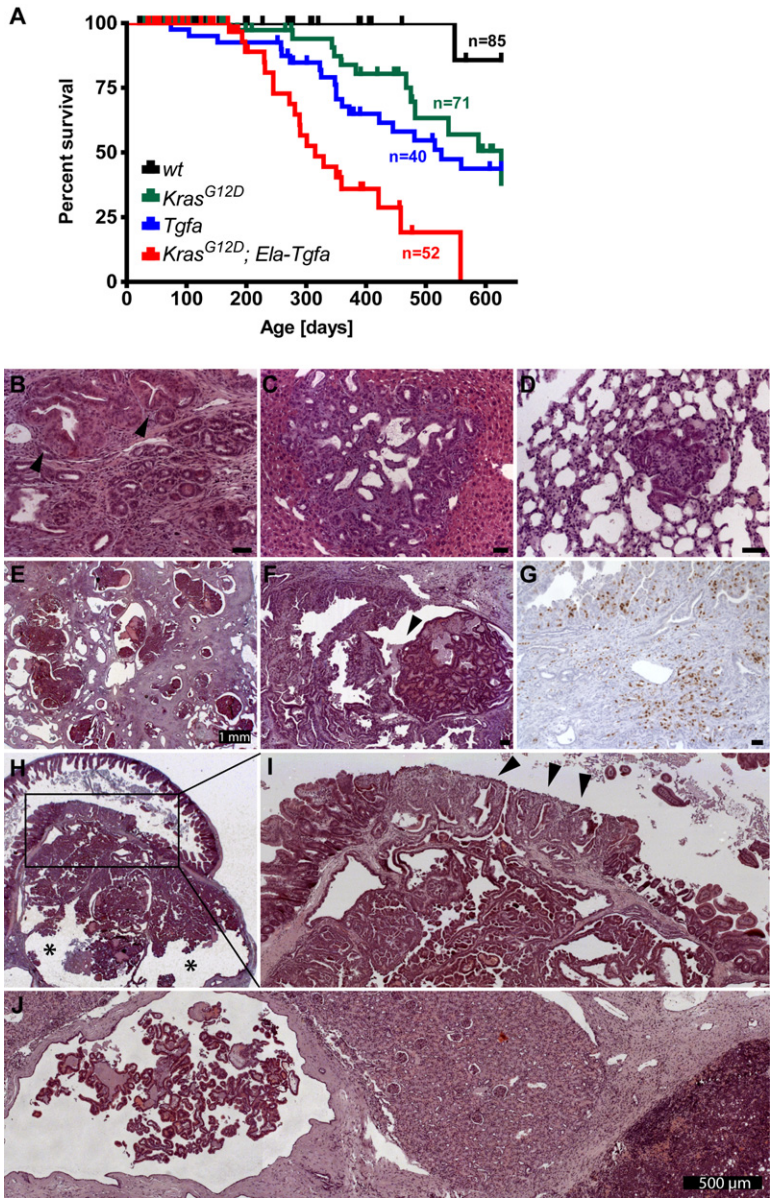

Figure 6. Survival Analysis and Progression of mPanIN and IPMN-like Precursor Lesions

(A) Kaplan-Meier curves show a significantly reduced survival time of *Kras*^{G12D};*Ela-Tgfa* mice compared to wild-type (WT, $p < 0.001$), *Kras*^{G12D} ($p < 0.001$), and *Ela-Tgfa* ($p = 0.002$) littermate controls.

(B–D) Metastatic PDAC of *Kras*^{G12D};*Ela-Tgfa* mice with mPanIN lesions (arrowheads) next to invasive cancer cells (B). Liver and lung metastasis showing similar glandular differentiation as the originating pancreatic tumor (C and D).

(E and F) Overview of a *Kras*^{G12D};*Ela-Tgfa* pancreas showing large IPMNs and fibrosis (E). Progression of IPMN-like lesions (F). Note transition of a normal appearing cystic papillary lesion into a lesion with highly abnormal architectural and nuclear properties (arrowhead).

(G) High proliferation of invasive PDAC with features of an IPMC as determined by Ki-67 immunostaining.

(H and I) Invasion of the adjacent duodenum by IPMN-like lesions (I, arrowheads). Note that the whole pancreas consists of papillary lesions (*).

(J) Renal metastasis resembling an IPMC in *Kras*^{G12D};*Ela-Tgfa* mice.

Scale bar is 50 μm or as shown.

lesions to PDAC; however, the development of metastatic PDAC occurs rather late and additional molecular alterations needed for malignant transformation and metastasis are not well defined. In this study we show that *Kras*^{G12D};*Ela-Tgfa* mice develop invasive and metastasizing PDAC significantly earlier than the single mutant models, resulting in a significantly reduced survival of *Kras*^{G12D};*Ela-Tgfa* mice. Moreover, moribund mice at the age of 6–8 months often present with disseminated metastasis suggesting concomitant action of mutant *Kras*^{G12D} and TGFα-induced Egfr signaling for the development of metastatic PDAC.

PDAC originates from preneoplastic precursor lesions, of which three morphologically distinct lesion types have been described: PanINs, the most common and best-characterized lesion type, and two cystic lesions, IPMN and MCN (Maitra et al., 2005). In *Kras*^{G12D};*Ela-Tgfa* mice, we observed the parallel development and progression of mPanIN and IPMN lesions. While mPanIN lesions in our model had the same morphological and immunohistological characteristics as mPanINs from *Kras*^{G12D} mice, evidence for a true IPMN lesion type in our model is substantiated from several observations: (1) morphologically, IPMN-like lesions from *Kras*^{G12D};*Ela-Tgfa* mice are highly similar to human IPMNs on a macroscopic and microscopic level; (2) their ductal and Mucin-producing phenotype is confirmed by positive PAS staining and expression of CK19 but not amylase; (3) on a molecular level, *Kras*^{G12D};*Ela-Tgfa* pancreata show a significantly increased GSEA score when compared to a human IPMN gene signature (Sato et al., 2004); (4) many genes upregulated in human IPMN tumors such as *Psca* are

A

	EGFR	HER2	p-ERK	p-AKT	p-STAT3	HES1
Pancreatobiliary (n=3)	1	0	0	1	3	1
Intestinal (n=3)	0	0	0	3	1	0
Gastric (n=3)	0	0	0	0	1	0
Oncocytic (n=3)	1	0	0	3	3	1

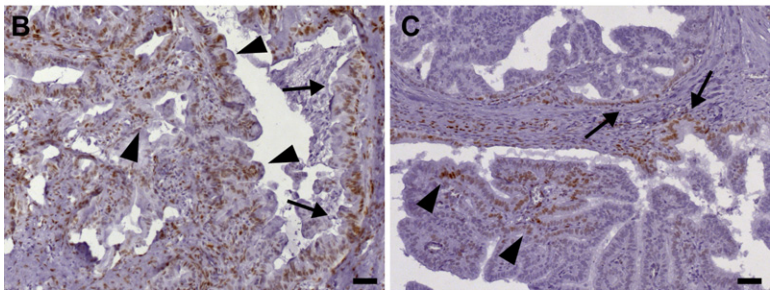

Figure 7. Signaling Pathways in Different Subtypes of Human IPMNs

(A–C) Human pancreatobiliary, intestinal, gastric, and oncocytic IPMNs (n = 3 for each subtype) were analyzed for expression of EGFR, HER2/neu, phospho-EKR, phospho-AKT, phospho-STAT3, and HES1. While phospho-AKT is found mainly in intestinal and oncocytic IPMNs, phospho-STAT3 (B) and HES1 (C) are expressed in nuclei of cyst lining (arrow) and papillary (arrowhead) cells of pancreatobiliary (B and C) and oncocytic IPMNs. Scale bar, 50 μm.

selectively upregulated in our model; (5) Egfr and Egfr-dependent effector pathways such as Stat3 are activated in both murine and human IPMN lesions and; (6) importantly, malignant transformation of IPMNs into invasive intraductal papillary mucinous carcinomas (IPMC) with invasion and metastasis occurred in a substantial fraction of *Kras*^{G12D}*;Ela-Tgfa* mice, a finding also observed in subsets of human IPMNs.

In humans, four subtypes of IPMNs have been proposed based on the morphological appearance and on immunohistochemical characteristics such as the MUC1, 2, and 5AC protein expression pattern. Based on these criteria, a gastric, intestinal, pancreatobiliary, and oncocytic subtype can be classified with the gastric-type IPMN involving mainly the branch ducts and the other subtypes involving predominantly the main duct (Furukawa et al., 2005). While the gastric-type IPMN is usually benign, the intestinal phenotype is associated with colloid (mucinous noncystic) carcinomas of usually better prognosis whereas the pancreatobiliary type of IPMN can proceed to invasive carcinomas mimicking usual and prognostic fatal PDAC (Adsay et al., 2002; Luttges et al., 2001). Applying this classification to our murine lesions shows a high correlation to the pancreatobiliary subtype of human IPMNs based on the morphological appearance, the MUC expression pattern, and the progression to metastatic PDAC.

Introduction of defined genetic alterations into mouse models of PDAC have allowed dissection of genetic pathways leading to cystic lesions. Mice overexpressing TGFα with inactivation of the *Ink4a/Arf* locus as well as COX-2 overexpressing mice under control of the K5 promoter developed serous cystadenoma (Bardeesy et al., 2002; Muller-Decker et al., 2006). Mucinous cystic tumors were recently described in mice with concomitant activation of *Kras*^{G12D} and inactivation of *Smad4*. In here, development of MCNs and IPMNs was reported in *p48*$^{Cre/+}$*;Kras*$^{LSL\text{-}G12D/+}$*;Dpc4*$^{flox/+}$ and *Ptf1a-Cre LSL-Kras*^{G12D} *Smad4*$^{lox/lox}$ mice, respectively (Bardeesy et al., 2006b; Izeradjene et al., 2007). These highly interesting findings demonstrate the importance of Smad4 for development of cystic precursor lesions; however, as human IPMCs only seldom harbor mutations in the *SMAD4* gene, additional pathways may be considered for IPMN and IPMC development. The invasive and metastatic nature of IPMCs found in *Kras*^{G12D}*;Ela-Tgfa* mice demonstrates a role of Egfr signaling in IPMN initiation and progression. Since IPMNs do not develop in *Kras*^{G12D} mice with or without additional inactivation of tumor suppressors such as *Tp53*, *p16Ink4a*, or *p19Arf* (Aguirre et al., 2003; Bardeesy et al., 2006a; Hingorani et al., 2003; Hingorani et al., 2005), we hypothesize that Tgfa-induced Egfr in synergy with Ras signaling initiates formation of papillary lesions while Kras^{G12D} activation has an accelerating effect. Accordingly, we find development of IPMN-like lesions in a small subset of old Ela-Tgfa mice as a consequence of Egfr signaling possibly in conjunction with sporadic *Kras* mutation. Our biochemical and immunohistochemical data support a role for Egfr activation, although tissue expression in murine and human preneoplastic and malignant IPMN lesions was variable, possibly because of low expression levels, a short half-life, or rapid recycling. Further support for a role of increased EGFR signaling in IPMN pathogenesis comes from a report showing synchronous expression of EGF and EGFR in all 11 malignant IPMNs but only in 1 of 18 malignant MCNs and 30 of 73 PDACs (Yeh et al., 2002, 2005).

Regarding the role of Egfr and Ras effectors involved in IPMN pathogenesis, we did not find evidence for selective activation of ERK1/2 or AKT in IPMN lesions; however, the

selectively increased expression of phospho-STAT3 protein and a *Stat3* gene signature in *Kras*^{G12D}*;Ela-Tgfa* mice provide evidence for an important role of this pathway in IPMN development. The finding of activated Stat3 signaling with increased expression of Bcl-xL occurring correlates well with a previously identified important role for STAT3 in human PDAC (Greten et al., 2002). Thus, a higher apoptotic resistance of precursor cells may be a possible mechanism for the induction of large preneoplastic papillary lesions. Moreover, Stat3 activation was recently described to be essential for the formation of acinoductal metaplasia, showing that Stat3 plays an important role in regulation of pancreatic cell fate and induction of pancreatic neoplasia (Miyatsuka et al., 2006).

As activation of Stat3 is not selective for IPMNs but is also found in PanIN lesions, it may also explain the accelerated progression of PanIN lesions compared to *Kras*^{G12D} mice. In fact, despite their different histological appearance, pancreatobiliary IPMNs and PanINs may share common molecular alterations. This hypothesis is underscored by expression profiling of these lesion subtypes revealing several upregulated genes found in PanINs, IPMNs, and PDACs, suggesting a common key signature for pancreatic ductal neoplasia (Sato et al., 2004). In humans, molecular alterations typically seen in PanINs such as *KRAS*, *p16INK4A*, *TP53*, or *DPC4/SMAD4* mutations have also been found in IPMNs, albeit at lower frequency (Biankin et al., 2002; Wada, 2002). The high degree of similarity in genetic alterations regarding the initial mutations in the progression from early to late PanIN development led us to hypothesize that some IPMN types may actually present as PanIN lesions in larger ducts sharing the same molecular pathogenesis and possibly the same cell of origin. Support for this hypothesis comes from several findings, including the observation that in some human pancreata PanINs are found in association with IPMNs (Biankin et al., 2004), a progression model for IPMNs similar to the one that has been described for progression of PanIN lesions and from the fact that PanINs may also involve large ducts while IPMNs can arise in smaller ducts (overview in Hruban et al., 2004). Most interestingly, a recent publication on the development of preneoplastic lesions in patients with a family history of PDAC reported a high occurrence of IPMN-like lesions in patients intensively screened for development of pancreatic abnormalities concluding that IPMNs may be part of the phenotypic spectrum of familial PDAC (Canto et al., 2006).

The histological appearance of invasive IPMC invading the duodenum, spleen, and kidneys as well as preliminary data showing differing expression of IPMN markers in cell lines derived from PDAC with IPMN features compared to PDAC cell lines from the *Kras*^{G12D} model (data not shown) strongly suggests development of PDAC from IPMN-like lesions at least in some of the *Kras*^{G12D}*;Ela-Tgfa* animals. The observation that some *Kras*^{G12D}*;Ela-Tgfa* pancreata with invasive IPMN tumors consisted almost completely of IPMN lesions while other mice had mPanIN-dominated pancreata suggests that cell lineages from which preneoplastic lesions develop are committed early to an IPMN or PanIN accentuated carcinogenesis. If both precursor lesions originate from the same cell of origin is a highly interesting yet not easily addressable question. Our findings of most IPMN-like lesions lacking acinar characteristics as well as the very low frequency of IPMN formation in *Ela-Cre-ER;Kras*^{G12D}*;Ela-Tgfa* mice argues against a terminally differentiated acinar cell as cell of origin. The finding of early HES1 expression at 7 days correlates well with earlier results showing expansion of undifferentiated HES1-expressing precursor cells as a consequence of Egfr activation (Miyamoto et al., 2003). Thus, IPMN-like lesions likely do not originate from Tgfa-induced acinoductal metaplastic cells. In addition, two findings argue against centroacinar cells as likely candidates for the development of IPMN lesions: the only moderately activated Akt-signaling pathway and the fact that, in contrast to recently described conditional PTEN knockout mice (Stanger et al., 2005), IPMN-like lesions can develop in *Ela-Cre-ER;Kras*^{G12D}*;Ela-Tgfa* mice, albeit at low frequency. Thus, we suggest IPMNs to originate from pancreatic progenitor cells, which may not only be activated cell-autonomously but also in a possible autocrine or paracrine manner, e.g., by stimulation of a potential stem cell niche.

The strong upregulation of nuclear HES1 in the early pancreas of *Kras*^{G12D}*;Ela-Tgfa* mice may be an indicator of increased Notch activation playing an important role in IPMN initiation and development. Interestingly, the missing or, at the most, much lower expression of SHH in IPMN lesions compared to mPanIN lesions in our model may suggest divergent roles of these cell fate-regulating pathways for precursor development. The well-described role of Hedgehog activation in PanINs (Pasca di Magliano et al., 2006; Prasad et al., 2005; Thayer et al., 2003) and the strong activation of Notch signaling in Tgfa-overexpressing models (Miyamoto et al., 2003) implies further studying the respective role of Notch and Hedgehog signaling in selective precursor lesion development.

In conclusion, this study demonstrates an important role of growth factors in pancreatic carcinogenesis. Overexpression of TGFα not only led to an acceleration of the PanIN-to-PDAC progression in the *Kras*^{G12D} model but also to the development of cystic papillary lesions reminiscent of human pancreatobiliary IPMNs. Increased expression of phosphorylated STAT3 and Bcl-xL as a result of synergistic Egfr and Kras^{G12D} signaling suggests an important role for this pathway in the carcinogenic process, while cell lineage experiments support the involvement and expansion of a progenitor cell population as possible cell of origin for the induction of IPMN lesions. In addition, the model presented here provides evidence for the hypothesis that different types of precursor lesions may occur on the same genetic background. Defining both the common and the differing molecular properties of each type of lesion may help to dissect these clinical entities and may provide a platform for further subtype-specific therapeutic approaches.

EXPERIMENTAL PROCEDURES

Mouse Strains

Kras$^{+/LSL\text{-}G12D}$, *Pdx1-Cre*, and *Elastase-Cre-ER* mice have been described before (Gu et al., 2002; Hingorani et al., 2003; Stanger et al., 2005). *Ptf1a*$^{+/Cre}$ knockin mice (termed *p48*$^{+/Cre}$ mice to distinguish them from previously described *Ptf1a-Cre* knockin mice [Kawaguchi et al., 2002]) were generated in our lab and are described in detail elsewhere (Nakhai et al., 2007). *Ela-Tgfa*-hGH mice have been described before (Sandgren et al., 1990; Wagner et al., 2001; Wagner et al., 1998). Mice were interbred to obtain *p48*$^{+/Cre}$; *Kras*$^{+/LSL\text{-}G12D}$; *Ela-Tgfa* (*Kras*^{G12D};*Ela-Tgfa*) animals on a mixed 129SV;C57BL/6 background. Wild-type, *p48*$^{+/Cre}$;*Kras*$^{+/LSL\text{-}G12D}$ (*Kras*^{G12D}) and *Ela-Tgfa* littermates were used as controls. All experiments were performed according to the guidelines of the local Animal Use and Care Committees.

Affymetrix Gene Chip Analysis and GSEA

Pancreata of four mice per genotype were dissected 7 days postnatally. Total RNA was prepared as described above. One to five micrograms of labeled RNA was hybridized to mouse expression gene chip arrays (Affymetrix Mouse Genome 430A 2.0 Array) according to Affymetrix protocols. Gene chips were scanned and analyzed using Affymetrix Microarray Suite 5.0 software (MAS 5.0).

For the IPMN signature gene set we matched the 643 transcripts listed on http://www.pathology2.jhu.edu/pancreas/IPMN to 513 unique transcript IDs from the Mouse Genome 430A 2.0 array. For the proliferation signature gene set (Whitfield et al., 2006), 40 out of 45 genes were matched.

GSEA software was provided by the Broad Institute of MIT and Harvard (http://www.broad.mit.edu/gsea/). We acknowledge the use of the gene set enrichment analysis and GSEA software (Subramanian et al., 2005). For both gene sets, we used the default parameters of the GSEA software package, except for the number of permutations (1000). Each genotype was tested against all other genotypes (WT, *Kras*^{G12D}, *Ela-Tgfa*, and *Kras*^{G12D};*Ela-Tgfa*).

Statistical Analyses

Kaplan-Meier curves were calculated using the survival time for each mouse from all littermate groups (WT, *Kras*^{G12D}, *Ela-Tgfa*, and *Kras*^{G12D}; *Ela-Tgfa*). The log-rank test was used to test for significant differences between the four groups. For gene expression analysis the unpaired two-tailed Student's t test was used. $p < 0.05$ was considered significant.

Histological, Molecular, and Biochemical Analyses

Detailed descriptions of procedures are provided in the Supplemental Data.

Supplemental Data

The Supplemental Data include Supplemental Experimental Procedures, one supplemental table, and five supplemental figures and can be found with this article online at http://www.cancercell.org/cgi/content/full/12/3/266/DC1/.

ACKNOWLEDGMENTS

We thank D.A. Tuveson, D.A. Melton, and E.P. Sandgren for the generous gift of transgenic mice and D.A. Tuveson for providing Mist1-Kras sections. We are grateful to O. Strobel and S. Thayer for supplying the Shh image. We thank J. Mages for his help in performing gene-profiling experiments and M. Neuhofer and C. Köhler for excellent technical assistance. This work was in part supported by grants from Deutsche Krebshilfe (#107195; J.T.S. and R.M.S.) and the Association for International Cancer Research (07-0543; J.T.S.).

Received: November 25, 2006
Revised: June 4, 2007
Accepted: August 3, 2007
Published: September 10, 2007

REFERENCES

Adsay, N.V., Merati, K., Andea, A., Sarkar, F., Hruban, R.H., Wilentz, R.E., Goggins, M., Iocobuzio-Donahue, C., Longnecker, D.S., and Klimstra, D.S. (2002). The dichotomy in the preinvasive neoplasia to invasive carcinoma sequence in the pancreas: Differential expression of MUC1 and MUC2 supports the existence of two separate pathways of carcinogenesis. Mod. Pathol. *15*, 1087–1095.

Aguirre, A.J., Bardeesy, N., Sinha, M., Lopez, L., Tuveson, D.A., Horner, J., Redston, M.S., and DePinho, R.A. (2003). Activated Kras and Ink4a/Arf deficiency cooperate to produce metastatic pancreatic ductal adenocarcinoma. Genes Dev. *17*, 3112–3126.

Allison, D.C., Piantadosi, S., Hruban, R.H., Dooley, W.C., Fishman, E.K., Yeo, C.J., Lillemoe, K.D., Pitt, H.A., Lin, P., and Cameron, J.L. (1998). DNA content and other factors associated with ten-year survival after resection of pancreatic carcinoma. J. Surg. Oncol. *67*, 151–159.

Bardeesy, N., Aguirre, A.J., Chu, G.C., Cheng, K.H., Lopez, L.V., Hezel, A.F., Feng, B., Brennan, C., Weissleder, R., Mahmood, U., et al. (2006a). Both p16(Ink4a) and the p19(Arf)-p53 pathway constrain progression of pancreatic adenocarcinoma in the mouse. Proc. Natl. Acad. Sci. USA *103*, 5947–5952.

Bardeesy, N., Cheng, K.H., Berger, J.H., Chu, G.C., Pahler, J., Olson, P., Hezel, A.F., Horner, J., Lauwers, G.Y., Hanahan, D., and Depinho, R.A. (2006b). Smad4 is dispensable for normal pancreas development yet critical in progression and tumor biology of pancreas cancer. Genes Dev. *20*, 3130–3146.

Bardeesy, N., Morgan, J., Sinha, M., Signoretti, S., Srivastava, S., Loda, M., Merlino, G., and DePinho, R.A. (2002). Obligate roles for p16(Ink4a) and p19(Arf)-p53 in the suppression of murine pancreatic neoplasia. Mol. Cell. Biol. *22*, 635–643.

Barton, C.M., Hall, P.A., Hughes, C.M., Gullick, W.J., and Lemoine, N.R. (1991). Transforming growth factor alpha and epidermal growth factor in human pancreatic cancer. J. Pathol. *163*, 111–116.

Biankin, A.V., Biankin, S.A., Kench, J.G., Morey, A.L., Lee, C.S., Head, D.R., Eckstein, R.P., Hugh, T.B., Henshall, S.M., and Sutherland, R.L. (2002). Aberrant p16(INK4A) and DPC4/Smad4 expression in intraductal papillary mucinous tumours of the pancreas is associated with invasive ductal adenocarcinoma. Gut *50*, 861–868.

Biankin, A.V., Kench, J.G., Biankin, S.A., Lee, C.S., Morey, A.L., Dijkman, F.P., Coleman, M.J., Sutherland, R.L., and Henshall, S.M. (2004). Pancreatic intraepithelial neoplasia in association with intraductal papillary mucinous neoplasms of the pancreas: Implications for disease progression and recurrence. Am. J. Surg. Pathol. *28*, 1184–1192.

Brugge, W.R., Lauwers, G.Y., Sahani, D., Fernandez-del Castillo, C., and Warshaw, A.L. (2004). Cystic neoplasms of the pancreas. N. Engl. J. Med. *351*, 1218–1226.

Canto, M.I., Goggins, M., Hruban, R.H., Petersen, G.M., Giardiello, F.M., Yeo, C., Fishman, E.K., Brune, K., Axilbund, J., Griffin, C., et al. (2006). Screening for early pancreatic neoplasia in high-risk individuals: A prospective controlled study. Clin. Gastroenterol. Hepatol. *4*, 766–781; quiz 665.

Friess, H., Guo, X.Z., Nan, B.C., Kleeff, O., and Buchler, M.W. (1999). Growth factors and cytokines in pancreatic carcinogenesis. Ann. N Y Acad. Sci. *880*, 110–121.

Furukawa, T., Kloppel, G., Volkan Adsay, N., Albores-Saavedra, J., Fukushima, N., Horii, A., Hruban, R.H., Kato, Y., Klimstra, D.S., Longnecker, D.S., et al. (2005). Classification of types of intraductal papillary-mucinous neoplasm of the pancreas: A consensus study. Virchows Arch. *447*, 794–799.

Greten, F.R., Weber, C.K., Greten, T.F., Schneider, G., Wagner, M., Adler, G., and Schmid, R.M. (2002). Stat3 and NF-kappaB activation prevents apoptosis in pancreatic carcinogenesis. Gastroenterology *123*, 2052–2063.

Grippo, P.J., Nowlin, P.S., Demeure, M.J., Longnecker, D.S., and Sandgren, E.P. (2003). Preinvasive pancreatic neoplasia of ductal phenotype induced by acinar cell targeting of mutant Kras in transgenic mice. Cancer Res. *63*, 2016–2019.

Gu, G., Dubauskaite, J., and Melton, D.A. (2002). Direct evidence for the pancreatic lineage: NGN3+ cells are islet progenitors and are distinct from duct progenitors. Development *129*, 2447–2457.

Guerra, C., Mijimolle, N., Dhawahir, A., Dubus, P., Barradas, M., Serrano, M., Campuzano, V., and Barbacid, M. (2003). Tumor induction by an endogenous K-ras oncogene is highly dependent on cellular context. Cancer Cell *4*, 111–120.

Hezel, A.F., Kimmelman, A.C., Stanger, B.Z., Bardeesy, N., and Depinho, R.A. (2006). Genetics and biology of pancreatic ductal adenocarcinoma. Genes Dev. *20*, 1218–1249.

Hingorani, S.R., Petricoin, E.F., Maitra, A., Rajapakse, V., King, C., Jacobetz, M.A., Ross, S., Conrads, T.P., Veenstra, T.D., Hitt, B.A., et al. (2003). Preinvasive and invasive ductal pancreatic cancer and its early detection in the mouse. Cancer Cell *4*, 437–450.

Hingorani, S.R., Wang, L., Multani, A.S., Combs, C., Deramaudt, T.B., Hruban, R.H., Rustgi, A.K., Chang, S., and Tuveson, D.A. (2005). Trp53R172H and KrasG12D cooperate to promote chromosomal instability and widely metastatic pancreatic ductal adenocarcinoma in mice. Cancer Cell *7*, 469–483.

Hruban, R.H., Adsay, N.V., Albores-Saavedra, J., Anver, M.R., Biankin, A.V., Boivin, G.P., Furth, E.E., Furukawa, T., Klein, A., Klimstra, D.S., et al. (2006). Pathology of genetically engineered mouse models of pancreatic exocrine cancer: Consensus report and recommendations. Cancer Res. *66*, 95–106.

Hruban, R.H., Takaori, K., Klimstra, D.S., Adsay, N.V., Albores-Saavedra, J., Biankin, A.V., Biankin, S.A., Compton, C., Fukushima, N., Furukawa, T., et al. (2004). An illustrated consensus on the classification of pancreatic intraepithelial neoplasia and intraductal papillary mucinous neoplasms. Am. J. Surg. Pathol. *28*, 977–987.

Izeradjene, K., Combs, C., Best, M., Gopinathan, A., Wagner, A., Grady, W.M., Deng, C.X., Hruban, R.H., Adsay, N.V., Tuveson, D.A., and Hingorani, S.R. (2007). Kras(G12D) and Smad4/Dpc4 Haploinsufficiency Cooperate to Induce Mucinous Cystic Neoplasms and Invasive Adenocarcinoma of the Pancreas. Cancer Cell *11*, 229–243.

Kawaguchi, Y., Cooper, B., Gannon, M., Ray, M., MacDonald, R.J., and Wright, C.V. (2002). The role of the transcriptional regulator Ptf1a in converting intestinal to pancreatic progenitors. Nat. Genet. *32*, 128–134.

Kosmahl, M., Pauser, U., Peters, K., Sipos, B., Luttges, J., Kremer, B., and Kloppel, G. (2004). Cystic neoplasms of the pancreas and tumor-like lesions with cystic features: A review of 418 cases and a classification proposal. Virchows Arch. *445*, 168–178.

Luttges, J., Zamboni, G., Longnecker, D., and Kloppel, G. (2001). The immunohistochemical mucin expression pattern distinguishes different types of intraductal papillary mucinous neoplasms of the pancreas and determines their relationship to mucinous noncystic carcinoma and ductal adenocarcinoma. Am. J. Surg. Pathol. *25*, 942–948.

Maitra, A., Fukushima, N., Takaori, K., and Hruban, R.H. (2005). Precursors to invasive pancreatic cancer. Adv. Anat. Pathol. *12*, 81–91.

Miyamoto, Y., Maitra, A., Ghosh, B., Zechner, U., Argani, P., Iacobuzio-Donahue, C.A., Sriuranpong, V., Iso, T., Meszoely, I.M., Wolfe, M.S., et al. (2003). Notch mediates TGF alpha-induced changes in epithelial differentiation during pancreatic tumorigenesis. Cancer Cell *3*, 565–576.

Miyatsuka, T., Kaneto, H., Shiraiwa, T., Matsuoka, T.A., Yamamoto, K., Kato, K., Nakamura, Y., Akira, S., Takeda, K., Kajimoto, Y., et al. (2006). Persistent expression of PDX-1 in the pancreas causes acinar-to-ductal metaplasia through Stat3 activation. Genes Dev. *20*, 1435–1440.

Muller-Decker, K., Furstenberger, G., Annan, N., Kucher, D., Pohl-Arnold, A., Steinbauer, B., Esposito, I., Chiblak, S., Friess, H., Schirmacher, P., and Berger, I. (2006). Preinvasive duct-derived neoplasms in pancreas of keratin 5-promoter cyclooxygenase-2 transgenic mice. Gastroenterology *130*, 2165–2178.

Nakhai, H., Sel, S., Favor, J., Mendoza-Torres, L., Paulsen, F., Duncker, G.I., and Schmid, R.M. (2007). Ptf1a is essential for the differentiation of GABAergic and glycinergic amacrine cells and horizontal cells in the mouse retina. Development *134*, 1151–1160.

Ohuchida, K., Mizumoto, K., Fujita, H., Yamaguchi, H., Konomi, H., Nagai, E., Yamaguchi, K., Tsuneyoshi, M., and Tanaka, M. (2006). Sonic hedgehog is an early developmental marker of intraductal papillary mucinous neoplasms: Clinical implications of mRNA levels in pancreatic juice. J. Pathol. *210*, 42–48.

Pasca di Magliano, M., Sekine, S., Ermilov, A., Ferris, J., Dlugosz, A.A., and Hebrok, M. (2006). Hedgehog/Ras interactions regulate early stages of pancreatic cancer. Genes Dev. *20*, 3161–3173.

Perou, C.M., Jeffrey, S.S., van de Rijn, M., Rees, C.A., Eisen, M.B., Ross, D.T., Pergamenschikov, A., Williams, C.F., Zhu, S.X., Lee, J.C., et al. (1999). Distinctive gene expression patterns in human mammary epithelial cells and breast cancers. Proc. Natl. Acad. Sci. USA *96*, 9212–9217.

Prasad, N.B., Biankin, A.V., Fukushima, N., Maitra, A., Dhara, S., Elkahloun, A.G., Hruban, R.H., Goggins, M., and Leach, S.D. (2005). Gene expression profiles in pancreatic intraepithelial neoplasia reflect the effects of Hedgehog signaling on pancreatic ductal epithelial cells. Cancer Res. *65*, 1619–1626.

Sandgren, E.P., Luetteke, N.C., Palmiter, R.D., Brinster, R.L., and Lee, D.C. (1990). Overexpression of TGF alpha in transgenic mice: Induction of epithelial hyperplasia, pancreatic metaplasia, and carcinoma of the breast. Cell *61*, 1121–1135.

Sato, N., Fukushima, N., Maitra, A., Iacobuzio-Donahue, C.A., van Heek, N.T., Cameron, J.L., Yeo, C.J., Hruban, R.H., and Goggins, M. (2004). Gene expression profiling identifies genes associated with invasive intraductal papillary mucinous neoplasms of the pancreas. Am. J. Pathol. *164*, 903–914.

Schneider, G., Siveke, J.T., Eckel, F., and Schmid, R.M. (2005). Pancreatic cancer: Basic and clinical aspects. Gastroenterology *128*, 1606–1625.

Siveke, J.T., and Schmid, R.M. (2005). Chromosomal instability in mouse metastatic pancreatic cancer–it's Kras and Tp53 after all. Cancer Cell *7*, 405–407.

Stanger, B.Z., Stiles, B., Lauwers, G.Y., Bardeesy, N., Mendoza, M., Wang, Y., Greenwood, A., Cheng, K.H., McLaughlin, M., Brown, D., et al. (2005). Pten constrains centroacinar cell expansion and malignant transformation in the pancreas. Cancer Cell *8*, 185–195.

Subramanian, A., Tamayo, P., Mootha, V.K., Mukherjee, S., Ebert, B.L., Gillette, M.A., Paulovich, A., Pomeroy, S.L., Golub, T.R., Lander, E.S., and Mesirov, J.P. (2005). Gene set enrichment analysis: A knowledge-based approach for interpreting genome-wide expression profiles. Proc. Natl. Acad. Sci. USA *102*, 15545–15550.

Thayer, S.P., di Magliano, M.P., Heiser, P.W., Nielsen, C.M., Roberts, D.J., Lauwers, G.Y., Qi, Y.P., Gysin, S., Fernandez-del Castillo, C., Yajnik, V., et al. (2003). Hedgehog is an early and late mediator of pancreatic cancer tumorigenesis. Nature *425*, 851–856.

Tuveson, D.A., Zhu, L., Gopinathan, A., Willis, N.A., Kachatrian, L., Grochow, R., Pin, C.L., Mitin, N.Y., Taparowsky, E.J., Gimotty, P.A., et al. (2006). Mist1-KrasG12D knock-in mice develop mixed differentiation metastatic exocrine pancreatic carcinoma and hepatocellular carcinoma. Cancer Res. *66*, 242–247.

Wada, K. (2002). p16 and p53 gene alterations and accumulations in the malignant evolution of intraductal papillary-mucinous tumors of the pancreas. J. Hepatobiliary Pancreat. Surg. *9*, 76–85.

Wagner, M., Greten, F.R., Weber, C.K., Koschnick, S., Mattfeldt, T., Deppert, W., Kern, H., Adler, G., and Schmid, R.M. (2001). A murine tumor progression model for pancreatic cancer recapitulating the genetic alterations of the human disease. Genes Dev. *15*, 286–293.

Wagner, M., Luhrs, H., Kloppel, G., Adler, G., and Schmid, R.M. (1998). Malignant transformation of duct-like cells originating from acini in transforming growth factor transgenic mice. Gastroenterology *115*, 1254–1262.

Warshaw, A.L., and Fernandez-del Castillo, C. (1992). Pancreatic carcinoma. N. Engl. J. Med. *326*, 455–465.

Whitfield, M.L., George, L.K., Grant, G.D., and Perou, C.M. (2006). Common markers of proliferation. Nat. Rev. Cancer *6*, 99–106.

Yeh, T.S., Jan, Y.Y., Chiu, C.T., Ho, Y.B., Chen, T.C., Lee, K.F., Chan, K.M., Hsu, J.C., Hwang, T.L., and Chen, M.F. (2002). Characterisation of oestrogen receptor, progesterone receptor, trefoil factor 1, and epidermal growth factor and its receptor in pancreatic cystic neoplasms and pancreatic ductal adenocarcinoma. Gut *51*, 712–716.

Yeh, T.S., Tseng, J.H., Liu, N.J., Chen, T.C., Jan, Y.Y., and Chen, M.F. (2005). Significance of cellular distribution of ezrin in pancreatic cystic neoplasms and ductal adenocarcinoma. Arch. Surg. *140*, 1184–1190.

Accession Numbers

Microarray data are available at ArrayExpress (http://www.ebi.ac.uk/arrayexpress; accession number E-TABM-304).